

Electronic Supplementary Information

Sonochemical Synthesis and Liquid Crystal Assembly of PS-*b*-PEO/Titania Aggregates

Yu Zhang, Hui Li, Yan-Qiong Liu and John Wang*

Department of Materials Science & Engineering, National University of Singapore,
Singapore 117574. E-mail: msewangj@nus.edu.sg

Experimental Section

Synthesis. In a typical synthesis process, 0.018 g polystyrene-*b*-poly(ethylene oxide) (PS-*b*-PEO, $M_n = 18000 \text{ g mol}^{-1}$ for PS and 7500 g mol^{-1} for PEO, with a polydispersity of 1.05, Polymer Source, Inc.) was first dissolved in 0.46 g tetrahydrofuran (THF, 99.9%, Fisher Scientific), a good solvent for both PS and PEO blocks, and stirred for 1 h. A colorless clear solution was obtained. 0.06 g titanium tetraisopropoxide (TTIP, 97%, Aldrich) and 1.25 g hydrochloric acid (HCl, 37%, Merck) were subsequently added dropwise into the solution. Molar ratios of these ingredients were controlled as follows: PS-*b*-PEO/THF/TTIP/HCl/H₂O = 0.001 : 9 : 0.3 : 1.8 : 6.21 (H₂O applied herein entirely arose from the 37% HCl solution). The system became orange-colored, translucent, and viscous because water arising from the 37% HCl solution is a precipitant for the PS blocks which induces aggregation of the PS blocks in the solution. After being stirred for another 3 h, the solution (defined as Sol_(I)) was sonicated for 2 h (defined as Sol_(II)) or 8 h (defined as Sol_(III)) in a ultrasound bath (Elma, E60H, 37 kHz), during which the bath was water-cooled to keep the temperature below 40 °C. The resultant solution was drop-casted on glass substrates followed by drying at ambient temperature and 67% relative humidity. After drying, the as-deposited layer was calcined at 500 °C for 2 h (1 °C min⁻¹ ramp) in air to remove the block copolymers and crystallize titania.

Fabrication of Dye-Sensitized Solar Cells (DSSCs). The 500 °C-calcined titania film deposited on a fluorine-doped tin oxide (FTO, TEC 15 from Dyesol, 3 mm thick, 80% transmittance in the visible, $15 \Omega \text{ sq}^{-1}$) substrate was immersed in anhydrous ethanol containing $5 \times 10^{-4} \text{ M}$ *cis*-bis(isothiocyanato)bis(2,2'-bipyridine-4,4'-dicarboxylato) ruthenium(II) bis-tetrabutylammonium (N719 dye, Solaronix) and kept for three days. It was then rinsed thoroughly with ethanol and dried. The Pt-coated FTO (Dyesol) was heated at 400 °C for 20 min in air before cell assembly. The electrolyte solution consisted of 0.6 M 1-butyl-3-methylimidazolium iodide (98%, Ionic Liquids Technology), 0.03 M iodine (99.5%), 0.1 M guanidine thiocyanate (99%), and 0.5 M 4-tert-butylpyridine (98%) in acetonitrile (99.8%)/valeronitrile (99.5%) (85/15, v/v). The titania photoanode and the Pt-coated FTO counter electrode were spaced and sealed by 25 μm thick thermoplast hot-melt sealing foil (SX1170-25, Solaronix). The electrolyte was introduced

with the help of one hole in the Pt-coated FTO via vacuum backfilling, and the hole was then sealed using SX1170-25 film. The cells had active areas of $0.2 - 0.4 \text{ cm}^2$.

As a comparison, a DSSC device was fabricated by screen-printing a commercially available titania paste (DSL 18NR-T from Dyesol, diameter of titania nanoparticles: $\sim 20\text{nm}$) on FTO (thickness of the titania layer: $8.5 \mu\text{m}$).

Characterization. CryoTEM (FEI Titan Krios, 300 kV), TEM (JEOL JEM 2010F, 200 kV), field emission SEM (Philips XL 30 FEG-SEM), and AFM (Veeco Metrology, MultiModeTM) were employed to investigate the morphology and texture of the samples. For TEM specimen preparation, if not specified otherwise, the samples were scratched off the substrate, suspended in ethanol, dropped onto a 200-mesh carbon-coated copper grid, and then dried at room temperature. For SEM specimen preparation, the sample was scratched off the glass substrate, and placed on a SEM holder with a carbon tape. No additional Au coating was required. The SEM was operated at an accelerating voltage of 15 kV and a working distance of 7.5 mm.

N_2 adsorption and desorption isotherms at -196°C were measured using a Micromeritics ASAP 2020 system. The samples that were scratched off the substrate were degassed at 200°C for 8 h. The Brunauer-Emmett-Teller (BET) surface area was estimated using adsorption data in a relative pressure range from 0.08 to 0.2. The total pore volume was calculated from the amount of N_2 adsorbed at a relative pressure of $P/P_0 = 0.965$. FTIR spectrophotometer (Varian 3100 Excalibur) was employed to identify the composition of the samples. XRD (Bruker AXS D8 Advance) measurements were carried out for identification of the crystalline phase of the samples. XRD phase analyses were conducted in a $\theta/2\theta$ Bragg-Brentano geometry, and 2θ varied from $20-70^\circ$. It was operated at 40 kV and 40 mA under Cu $\text{K}\alpha$ radiation (1.5406 \AA) with a step size of 0.04° and a time per step of 10 s.

Photocurrent-voltage measurements of the solar cells were performed using a Keithley 2420 sourcemeter. The irradiance source was a 150W NREL traceable Oriel Class AAA solar simulator (Model 92250A-1000). The output power was calibrated by a NREL traceable monocrystalline silicon reference cell (PVM 191) coupled with Newport Oriel PV reference cell system (Model 91150).

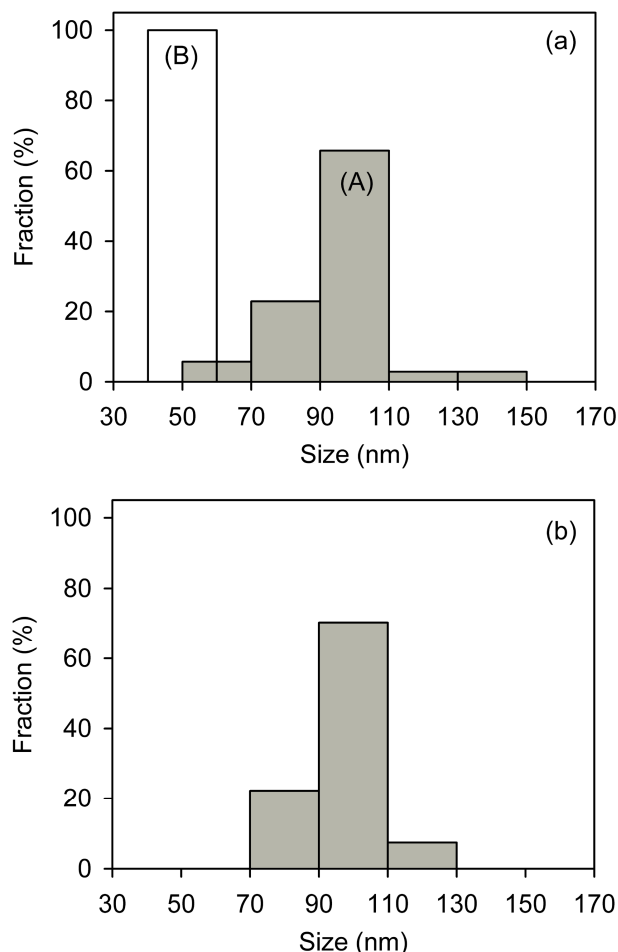


Fig. S1 (a) Size distribution histograms of (A) the vesicles in Sol_(II) and (B) the spherical micelles in Sol_(III), by analyses of the cryoTEM images. (b) Size distribution histogram of the as-deposited PS-*b*-PEO/titania film derived from Sol_(II), measured from SEM images. According to the size distribution histograms shown in Fig. S1a(A) and Fig. S1b, the size homogeneity of vesicles is still unsatisfactory, which ranges broadly from 50 to 150 nm, and the majority of vesicles falls into a size range of 90 – 110 nm. It agrees well with what were shown in Fig. 1c and Fig. 2d, where very small (~55 nm) and very big (~140 nm) vesicles were viewed.

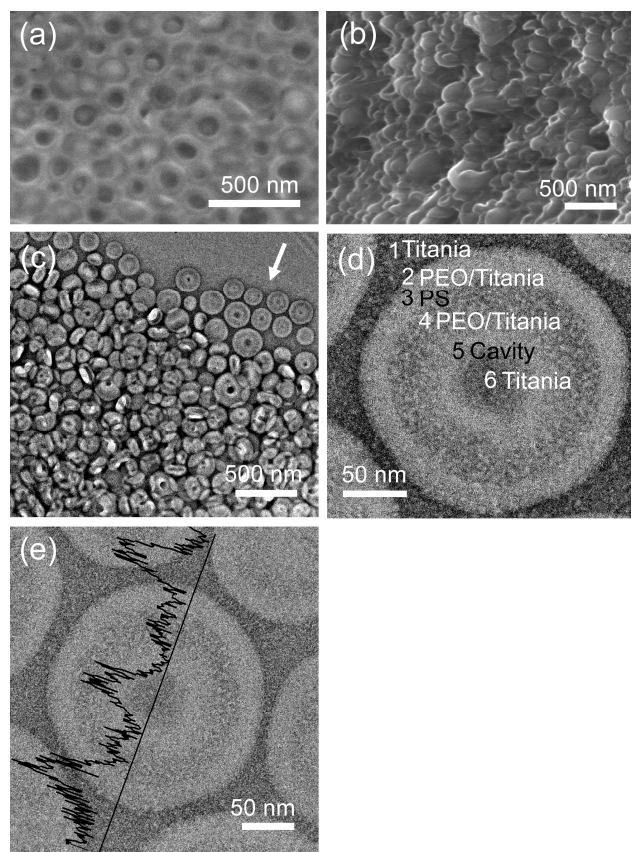


Fig. S2 Sol_(I) was drop-cast on glass substrates followed by drying at ambient temperature and 67% relative humidity. (a) SEM (Top view), (b) SEM (cross-sectional view), and (c)–(e) TEM images (at different magnifications) of the as-deposited PS-*b*-PEO/titania hybrids derived from Sol_(I). SEM images show bowl-shaped opening vesicles each with a solid core in the cavity. These vesicles are embedded in a continuous solid network in three dimensions. The TEM specimen preparation follows a different procedure, where Sol_(I) was dropped directly on a TEM Cu grid, and excess solution was removed by touching the grid edge using a Kimwipe delicate wipe. Because of such preparation procedures, the as-deposited layer on the Cu grid contains local ultrathin areas (as marked by an arrow in (c)), which may be viewed as being composed of individually dispersed vesicles. EDX line scan spectrum in (e) shows the distribution of titanium element in the bowl-shaped opening vesicles. It confirms that the dark regions are composed of titanium species which have a higher electron density than polymers.

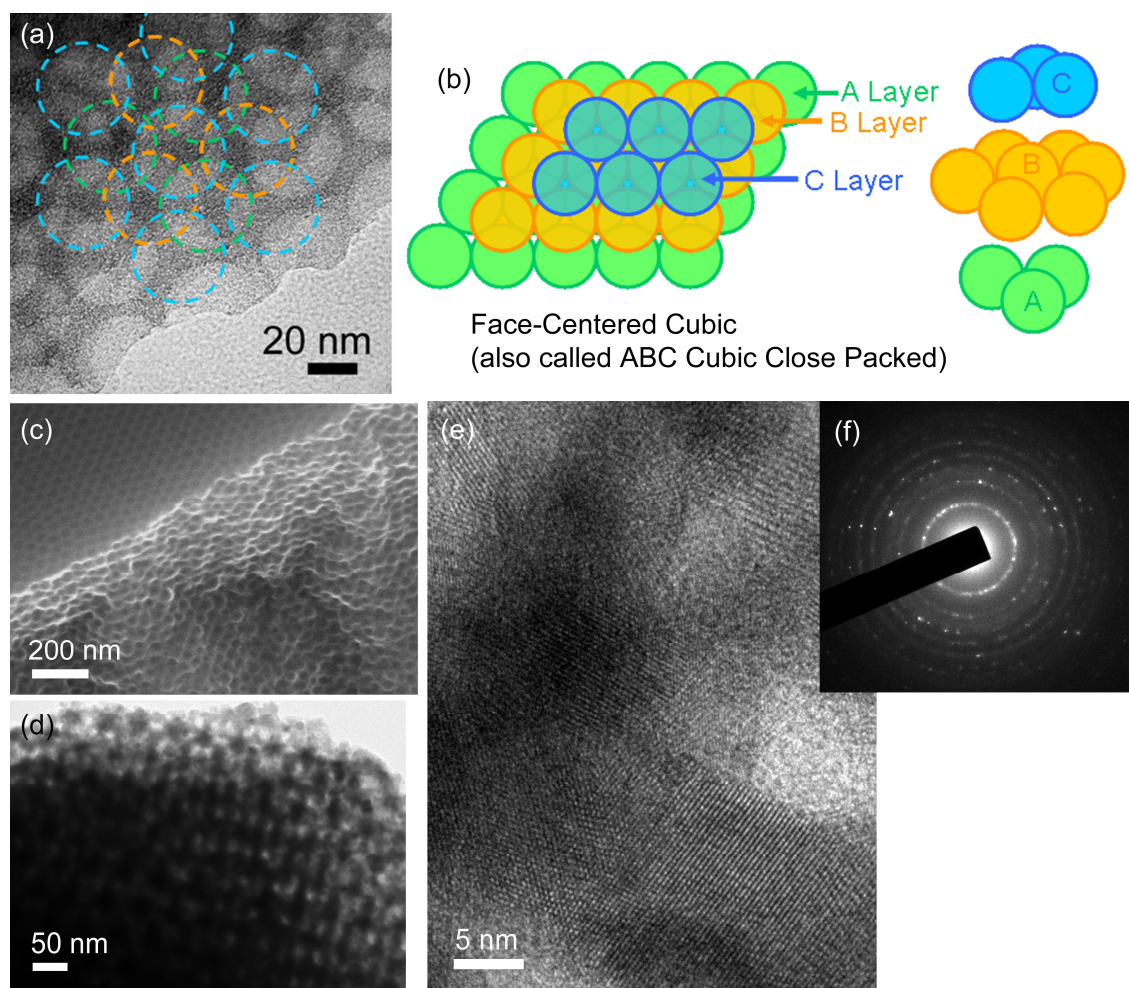


Fig. S3 (a) TEM image of the as-deposited PS-*b*-PEO/titania hybrid film derived from Sol_(III). (b) Schematic illustration of the face-centered cubic arrangement of spherical micelles. (c) Enlarged cross-sectional SEM image of the as-deposited PS-*b*-PEO/titania hybrid film derived from Sol_(III). (d) TEM and (e) high resolution TEM images of the corresponding sample upon calcination at 500 °C. (f) is the selected area diffraction pattern of (d).

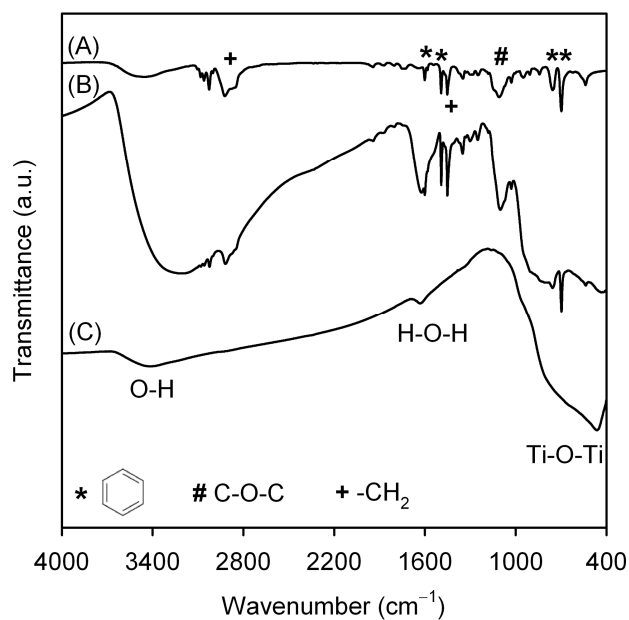


Fig. S4 FTIR transmittance spectra of (A) PS-*b*-PEO, (B) the as-deposited PS-*b*-PEO/titania film derived from Sol_(II), and (C) the corresponding sample upon calcination at 500 °C. (A): The four bands centered at 700, 760, 1490, and 1600 cm^{-1} , characteristic of the benzene ring, and the broad band centered at 1115 cm^{-1} , assigned to the stretching vibration of C-O-C ($\nu_{\text{C-O-C}}$), confirm the presence of PS and PEO blocks, respectively. The bands at 3000–2800 cm^{-1} and 1485 – 1330 cm^{-1} regions are assigned to the stretching vibration (ν_{CH}) and bending vibration (δ_{CH}) of CH₂ groups, respectively. (B): Besides the bands arising from PS-*b*-PEO, two large bands centered at ~3350 and 1640 cm^{-1} , assigned to the stretching vibration of O-H (ν_{OH}) and the bending vibration of H-O-H (δ_{OH}), respectively, are observed for the as-deposited PS-*b*-PEO/titania film. They reveal that a large number of structure or surface hydroxyl groups and hydroxyl groups from physisorbed water exist in the hybrids. Another broad low-frequency band in the range of 400–1000 cm^{-1} is observed for the hybrids, which corresponds to the ν_{TiOTi} of the inorganic framework. The low intensity suggests a low degree of condensation of the inorganic framework. (C): Upon calcination at 500 °C, the intensity of the Ti-O-Ti vibration band increases, demonstrating an enhanced condensation as the thermal treatment proceeds. In addition, the bands characteristic of hydroxyl groups fade upon thermal treatment, but are still prominent even after calcination at 500 °C. It indicates the presence of surface hydroxyl groups probably in the Ti-OH form. The bands corresponding to the block copolymers disappear at 500 °C, indicating an almost complete removal of the copolymer templates.

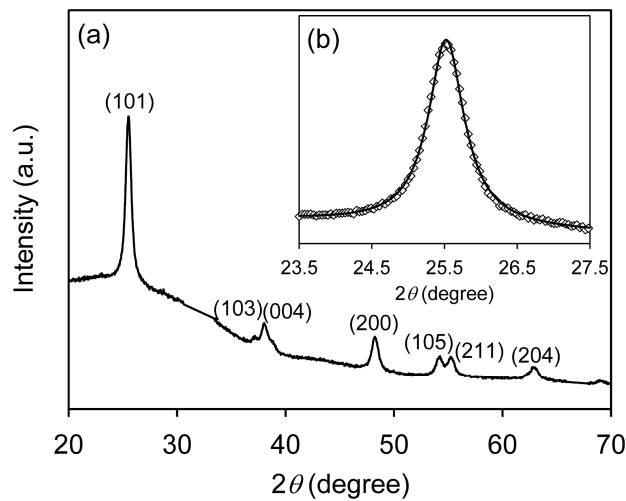


Fig. S5 (a) XRD pattern of the 500 °C-calcined film derived from Sol_(II). The diffraction peaks can be ascribed to the (101), (103), (004), (200), (105), (211), and (204) planes of anatase phase. (b) Full width at half maximum (fwhm) of the (101) peak was obtained by fitting to Lorentz distribution. The dots are for the experimental data and the full curves are fit to Lorentzian distribution. Calculation of the peak width using the Scherrer equation yielded an average crystallite size of 13.6 nm.

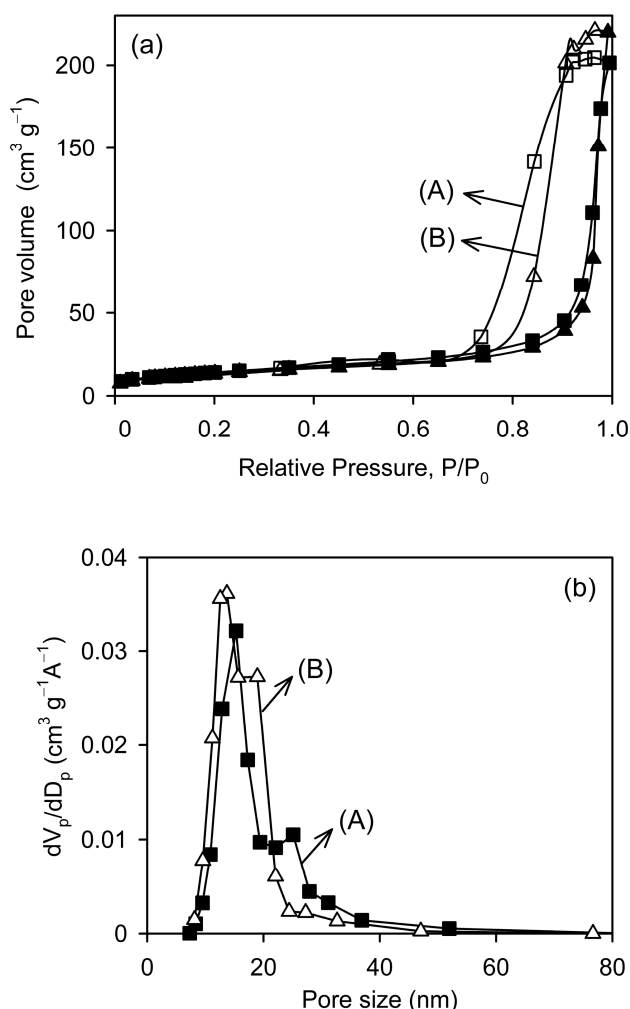


Fig. S6 (a) N_2 adsorption-desorption isotherms of (A) the vesicular porous titania derived from Sol_(II), and (B) the *fcc* mesoporous titania derived from Sol_(III), upon calcination at 500°C . Solid and open symbols denote adsorption and desorption branches, respectively. For curve (A), the relatively sharp adsorption branch reflects uniform pore sizes. However, the desorption branch shows a broad step and is located far from the adsorption branch; it features the specific vesicular porous structure with less-uniform and small pore connections. The BET surface area and pore volume for the vesicular porous titania were measured to be $51.1 \text{ m}^2 \text{ g}^{-1}$ and $0.32 \text{ cm}^3 \text{ g}^{-1}$, respectively. Curve (B) shows typical type IV isotherm curves. A steep adsorption branch was observed indicating a superior uniformity of mesopores. The desorption branch is also steep and located close to the adsorption branch, revealing that the mesopores are interconnected via uniform large windows which agrees well with the TEM observations (Fig. 3g). The *fcc* mesoporous titania has surface area and pore volume of $52.0 \text{ m}^2 \text{ g}^{-1}$ and $0.36 \text{ cm}^3 \text{ g}^{-1}$, respectively. (b) BJH pore size distributions of (A) the vesicular porous titania and (B) the *fcc* mesoporous titania. The pore size distributions were calculated from the desorption branches of N_2 isotherms. Both the

vesicular and the *fcc* porous titania exhibit bimodal pore size distributions confirming the hierarchical porous structures.

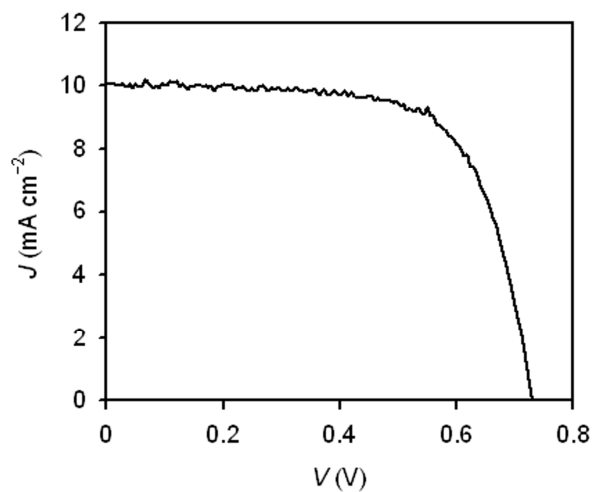


Fig. S7 Current-voltage curve of N719-sensitized DSSC derived from the 500 °C-calcined vesicular titania of 8.6 μm thick. The solar test was operated under simulated AM 1.5 solar illumination at an intensity of 100 mW cm⁻². The cell had an active area of 0.244 cm². The solar cell efficiency (η), short circuit current density (J_{SC}), open circuit voltage (V_{OC}), and fill factor (FF) were 5.14%, 10.06 mA cm⁻², 0.73 V, and 70.0%, respectively.

Table S1 Photovoltaic performance of the N719-sensitized DSSCs derived from the 500 °C-calcined vesicular porous titania and the *fcc* mesoporous titania of varying thicknesses. In the thickness range tested, all V_{OC} , J_{SC} , and FF increase and thus η increases with increasing titania thickness. The increases in V_{OC} and FF are ascribed to a reduced current leakage due to a better coverage of the FTO substrates with thicker titania layers. The increase in J_{SC} is ascribed to an increased amount of total surface area of the system and thereby an increased uptake of dyes with the increasing titania thickness. The vesicular porous titania outperforms the commercial titania of identical thickness (~8.5 μm) in both short circuit current and efficiency. This could well be attributed to the bicontinuous structure of the vesicular porous titania (an interconnected titania skeleton desirable for an efficient charge carrier transport and an interconnected pore system beneficial to the electrolyte diffusion).

Morphology	Thickness (μm)	V_{OC} (V)	J_{SC} (mA cm ⁻²)	FF (%)	η (%)
Vesicular Porous Titania	4.4	0.70	4.37	62.8	1.92
	5.6	0.72	6.65	68.3	3.29
	8.6	0.73	10.06	70.0	5.14
<i>fcc</i> Mesoporous Titania	3.0	0.70	3.96	58.6	1.63
	4.7	0.76	7.02	67.6	3.60
Commercial Titania Paste	8.5	0.73	8.37	66.9	4.07

Acknowledgement

This work was supported by the Agency for Science, Technology and Research, A-Star (Grant 0721010013), Singapore, and the Ministry of Education (MOE, URC Grant R284-000-054-112), conducted at the National University of Singapore.